Exotic nuclear properties in DRHBc

Youngman Kim
CENS/IBS

Introduction of IBS

4
Institutes

30
Research Centers

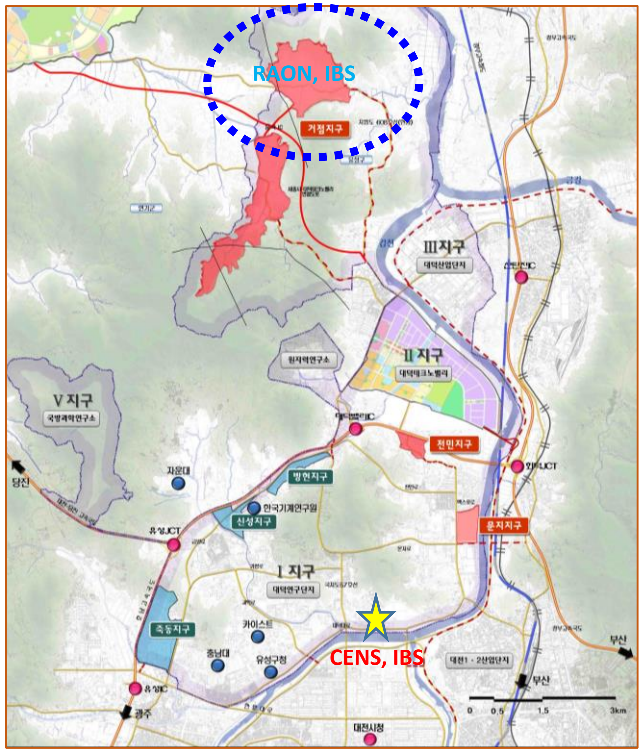


DCC1
DCC2
IBS

Introduction of IBS and CENS

Introduction and organization of CENS

Visions

CENS CENTER FOR EXOTIC NUCLEAR STUDIES

- To become one of the leading research institutions in nuclear physics
- To explore uncharted regions of nuclei and find important discoveries

- Nuclearsynthesis
- r-process/rp-process
- Origin of elements
- Nuclear properties of key nuclei
- Direct and indirect measurements

- Reaction mechanism
- Spin-isospin collectives
- Mass measurements
- Transmutation
- Dripline and new isotopes

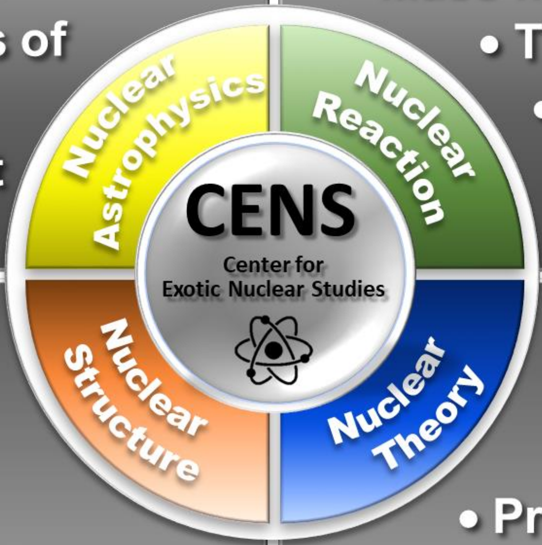

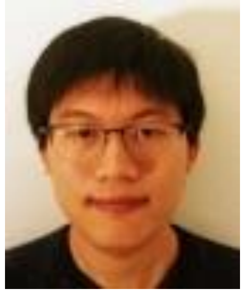

- Nuclear shell evolution
- Shape evolution
- Shape coexistence
- Isospin symmetry

- Compound and direct nuclear reaction
- Precise numerical quantum many-body calculations
- Density functional theory

- Interdisciplinary collaborations
- Research using RAON facility with ISOL and IF method
- Detector development

- RCHB (spherical symmetry)
- DRHBc (axial symmetry)
    - Dripline
    - Shape coexistence
    - Bubble
    - Alpha decay
    - Halos

RCHB

Lagrangian density of the point-coupling model

$$\mathcal{L} = \mathcal{L}^{free} + \mathcal{L}^{4f} + \mathcal{L}^{hot} + \mathcal{L}^{der} + \mathcal{L}^{em}$$

$$\mathcal{L}^{\rm free} = \bar\psi(i\gamma_\mu\partial^\mu - m)\psi,$$

$$\mathcal{L}^{\rm 4f} = -\tfrac{1}{2}\alpha_S(\bar\psi\psi)(\bar\psi\psi) - \tfrac{1}{2}\alpha_V(\bar\psi\gamma_\mu\psi)(\bar\psi\gamma^\mu\psi) - \tfrac{1}{2}\alpha_{TS}(\bar\psi\vec\tau\psi)(\bar\psi\vec\tau\psi) - \tfrac{1}{2}\alpha_{TV}(\bar\psi\vec\tau\gamma_\mu\psi)(\bar\psi\vec\tau\gamma^\mu\psi),$$

$$\mathcal{L}^{\rm hot} = -\tfrac{1}{3}\beta_S(\bar\psi\psi)^3 - \tfrac{1}{4}\gamma_S(\bar\psi\psi)^4 - \tfrac{1}{4}\gamma_V[(\bar\psi\gamma_\mu\psi)(\bar\psi\gamma^\mu\psi)]^2,$$

$$\mathcal{L}^{\rm der} = -\tfrac{1}{2}\delta_S\partial_\nu(\bar\psi\psi)\partial^\nu(\bar\psi\psi) - \tfrac{1}{2}\delta_V\partial_\nu(\bar\psi\gamma_\mu\psi)\partial^\nu(\bar\psi\gamma^\mu\psi) - \tfrac{1}{2}\delta_{TS}\partial_\nu(\bar\psi\vec\tau\psi)\partial^\nu(\bar\psi\vec\tau\psi) - \tfrac{1}{2}\delta_{TV}\partial_\nu(\bar\psi\vec\tau\gamma_\mu\psi)\partial^\nu(\bar\psi\vec\tau\gamma_\mu\psi),$$

$$\mathcal{L}^{\rm em} = -\frac{1}{4}F^{\mu\nu}F_{\mu\nu} - e\frac{1-\tau_3}{2}\bar\psi\gamma^\mu\psi A_\mu.$$

After taking the mean field approximation on the above Lagrangian and performing the Legendre transformation, we obtain the corresponding mean field Hamiltonian:

$$E_{\rm RMF} = \langle\Phi|\mathcal{H}_{\rm RMF}|\Phi\rangle.$$

$|\Phi\rangle$ is the ground state of a nucleus

$$|\Phi\rangle = \prod_{a=1} c_a^\dagger|0\rangle,$$

$$\psi(x) = \sum_a \psi_a(x)c_a$$

By minimizing the density functional with respect to the densities,

Relativistic Dirac-Hartree-Bogoliubov equation

Kucharek and Ring, Z. Phys. A 339, 23 (1991)

$$\begin{pmatrix} h_D - \lambda & \Delta \\ -\Delta^* & -h_D^* + \lambda \end{pmatrix} \begin{pmatrix} U_k \\ V_k \end{pmatrix} = E_k \begin{pmatrix} U_k \\ V_k \end{pmatrix}$$

Dirac Hamiltonian

$$h_D = \boldsymbol{\alpha} \cdot \boldsymbol{p} + \beta(M + S(r)) + V(r)$$

where scalar and vector potentials

$$S(r) = \alpha_S \rho_S + \beta_S \rho_S^2 + \gamma_S \rho_S^3 + \delta_S \Delta_{\rho S}$$

$$V(r) = \alpha_V \rho_V + \gamma_V \rho_V^3 + \delta_V \Delta_{\rho V} + eA_0 + \alpha_{TV} \tau_3 \rho_{TV} + \delta_{TV} \tau_3 \Delta_{TV}$$

with local densities

$$\rho_S = \sum_{k>0} \bar{V}_k(r) V_k(r)$$

$$\rho_V = \sum_{k>0} V_k^+(r) V_k(r)$$

$$\rho_{TV} = \sum_{k>0} V_k^+(r) \tau_3 V_k(r)$$

The point-coupling constants and pairing strengths of PC-PK1 set.

Coupling constant	Value	Dimension
α_S	-3.96291×10^{-4}	MeV^{-2}
β_S	8.6653×10^{-11}	MeV^{-5}
γ_S	-3.80724×10^{-17}	MeV^{-8}
δ_S	-1.09108×10^{-10}	MeV^{-4}
α_V	2.6904×10^{-4}	MeV^{-2}
γ_V	-3.64219×10^{-18}	MeV^{-8}
δ_V	-4.32619×10^{-10}	MeV^{-4}
α_{TV}	2.95018×10^{-5}	MeV^{-2}
δ_{TV}	-4.11112×10^{-10}	MeV^{-4}
V_n	-349.5	$MeV\ fm^3$
V_p	-330.0	$MeV\ fm^3$

fitted to observables of 60 selected spherical nuclei, including the binding energies, charge radii, and empirical pairing gaps.

Zhao, Li, Yao, Meng, PRC 82, 054319 (2010)

The pairing potential reads,

$$\Delta_{kk'}(\mathbf{r},\mathbf{r}') = -\sum_{\tilde{k}\tilde{k}'} \mathbf{V}_{kk',\tilde{k}\tilde{k}'}(\mathbf{r},\mathbf{r}')\kappa_{\tilde{k}\tilde{k}'}(\mathbf{r},\mathbf{r}')$$

with the pairing tensor $\kappa = U^* V^T$ and a density-dependent delta pairing force

$$V^{pp}(\mathbf{r_1},\mathbf{r_2}) = V_0\delta(\mathbf{r_1}-\mathbf{r_2})\frac{1}{4}(1-P^\sigma)(1-\frac{\rho(\mathbf{r_1})}{\rho_0}).$$

V_0 = 685 MeV fm^3: fixed by experimental odd-even mass differences of Ca isotopes, Sn isotopes, N=20 isotones and N=50 isotones.

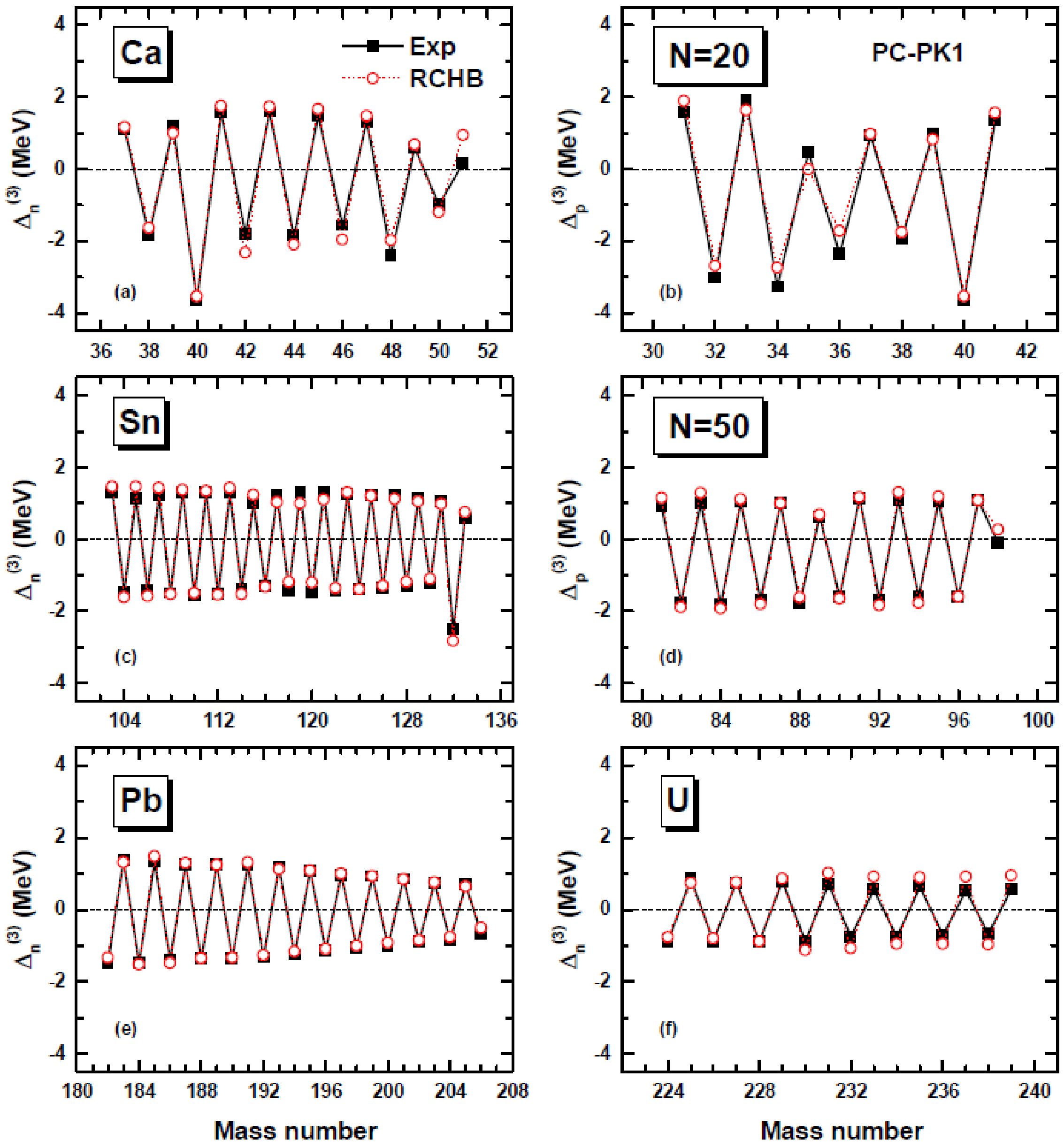

Ca
Exp
RCHB
N=20
PC-PK1
Sn
N=50
Pb
U
(a)
(b)
(c)
(d)
(e)
(f)
$\Delta_n^{(3)}$ (MeV)
$\Delta_p^{(3)}$ (MeV)
Mass number

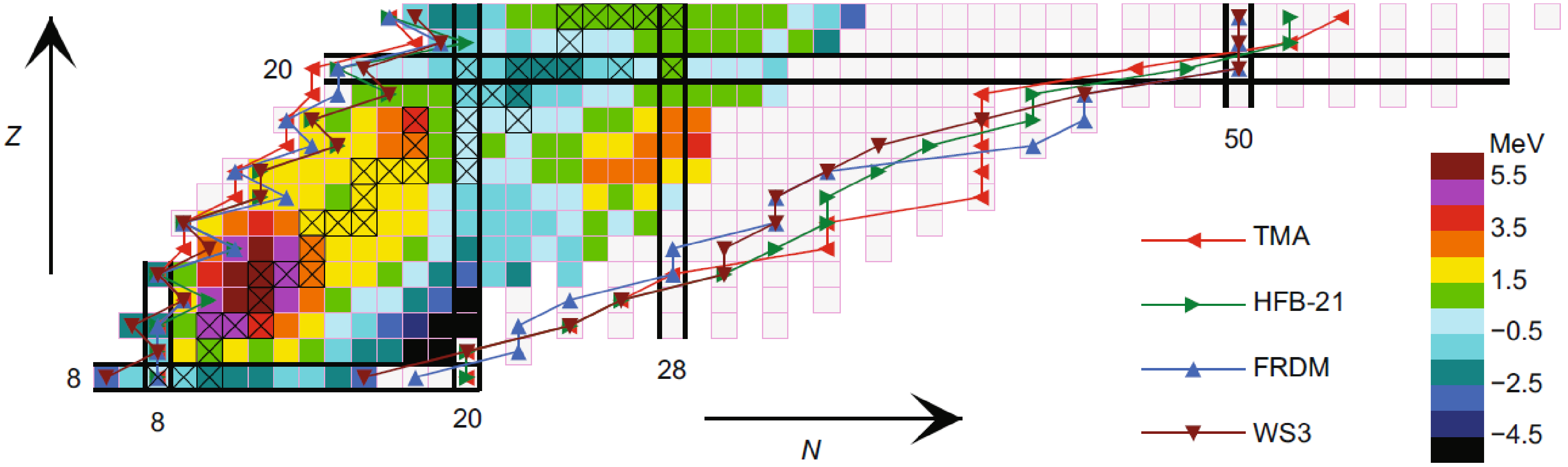

Figure 1 402 nuclei from O to Ti predicted to be bound by the RCHB theory with the covariant density functional PC-PK1. For 234 nuclei with the available data, the binding energy differences $E_b^{Exp.} - E_b^{Cal.}$ between the data [63] and present calculations are shown as different color. Furthermore, the nucleon drip-lines predicted by the mass tables TMA, HFB-21, FRDM and WS3 are plotted for comparison.

Mostly, due to consistent treatment of pairing correlations in the continuum, the neutron drip line predicted by RCHB theory are more neutron-rich than other mass models.

QU XiaoYing, CHEN Ying, ZHANG ShuangQuan, ZHAO PengWei, SHIN Ik Jae, LIM Yeunhwan, KIM Youngman &MENG Jie

Number of neutron-rich nuclei predicted to be bound by the RCHB, but unbound in the FRDM.

Element (Z)	ΔN	Element (Z)	ΔN	Element (Z)	ΔN	Element (Z)	ΔN	Element (Z)	ΔN
O (8)	2	Ni (28)	6	Rh (45)	11	Dy (66)	25	Fr (87)	29
Ne (10)	10	Cu (29)	6	Pd (46)	13	Ho (67)	23	Ra (88)	28
Na (11)	10	Zn (30)	1	Ag (47)	9	Er (68)	24	Ac (89)	28
Mg (12)	6	Ga (31)	1	Cd (48)	6	Tm (69)	26	Th (90)	37
Al (13)	8	Ge (32)	2	In (49)	4	Yb (70)	20	Pa (91)	43
Si (14)	6	As (33)	1	Sn (50)	6	Lu (71)	21	U (92)	39
P (15)	8	Se (34)	6	Sb (51)	8	Hf (72)	21	Np (93)	38
S (16)	6	Br (35)	7	Te (52)	2	Ta (73)	19	Pu (94)	44
K (19)	14	Kr (36)	9	I (53)	1	W (74)	13	Am (95)	45
Ca (20)	10	Rb (37)	10	Xe (54)	1	Re (75)	16	Cm (96)	38
Sc (21)	10	Sr (38)	14	Pr (59)	20	Os (76)	6	Bk (97)	38
Ti (22)	12	Y (39)	21	Nd (60)	16	Ir (77)	6	Cf (98)	37
V (23)	10	Zr (40)	19	Pm (61)	15	Pt (78)	6	Es (99)	35
Cr (24)	10	Nb (41)	12	Sm (62)	19	Au (79)	2	Fm (100)	36
Mn (25)	8	Mo (42)	12	Eu (63)	22	Hg (80)	2	Md (101)	28
Fe (26)	5	Tc (43)	13	Gd (64)	25	Tl (81)	2	No (102)	28
Co (27)	4	Ru (44)	10	Tb (65)	27	Rn (86)	31	Lr (103)	28

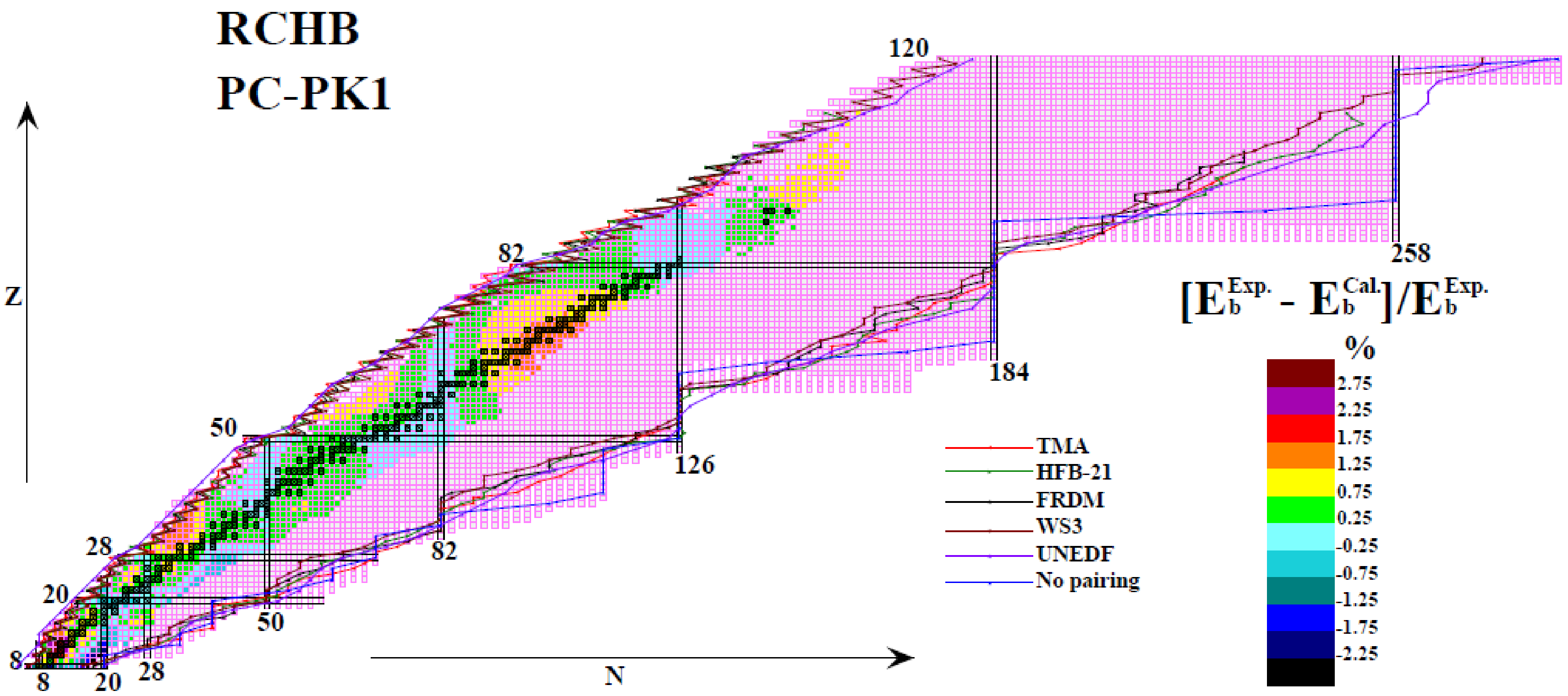

9035 bound nuclei in O(Z=8) to Z=120 region predicted by RCHB theory with PC-PK1. For 2231 observed nuclei, the relative binding energy differences between the data and present calculations are shown in different colors.
For measured nuclei, the root of relative square deviation:

$$\delta = \sum_i^N \sqrt{\frac{(E_b^{Exp.} - E_b^{Cal.})^2/(E_b^{Exp})^2}{N}} \text{ is } 0.70\%.$$

Atomic Data and Nuclear Data Tables 121–122 (2018) 1–215

Contents lists available at ScienceDirect

Atomic Data and Nuclear Data Tables

journal homepage: www.elsevier.com/locate/adt

The limits of the nuclear landscape explored by the relativistic continuum Hartree–Bogoliubov theory

X.W. Xia[a], Y. Lim[b,c], P.W. Zhao[d,e], H.Z. Liang[f], X.Y. Qu[a,g], Y. Chen[d,h], H. Liu[d], L.F. Zhang[d], S.Q. Zhang[d], Y. Kim[c], J. Meng[d,a,i,*]

[a] School of Physics and Nuclear Energy Engineering, Beihang University, Beijing 100191, China
[b] Cyclotron Institute, Texas A&M University, College Station, TX 77843, USA
[c] Rare Isotope Science Project, Institute for Basic Science, Daejeon 305-811, Republic of Korea
[d] State Key Laboratory of Nuclear Physics and Technology, School of Physics, Peking University, Beijing 100871, China
[e] Physics Division, Argonne National Laboratory, Argonne, IL 60439, USA
[f] RIKEN Nishina Center, Wako 351-0198, Japan
[g] School of Mechatronics Engineering, Guizhou Minzu University, China
[h] Institute of materials, China Academy of Engineering Physics, Sichuan, 621907, China
[i] Department of Physics, University of Stellenbosch, Stellenbosch, South Africa

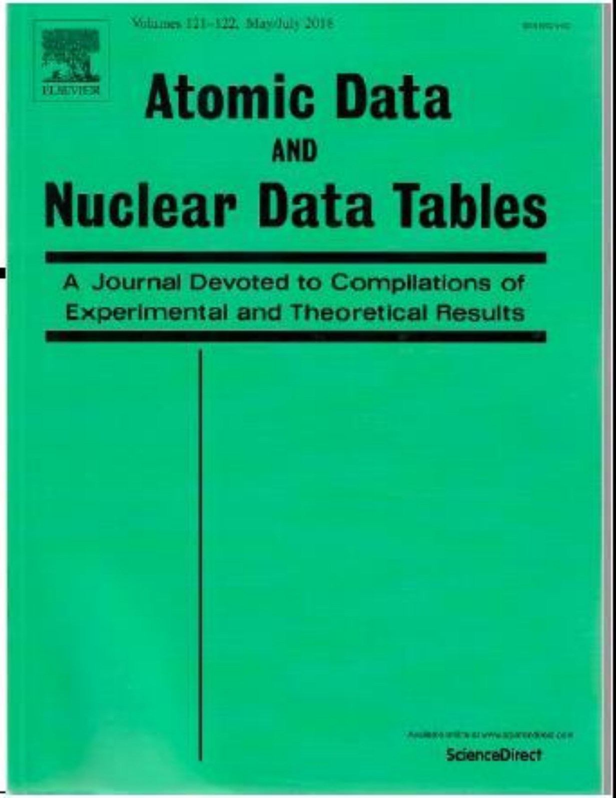

DRHBc mass table project

- ✓ To develop the DRHBc theory and extend it to provide a unified description of all even-even, odd-A, and odd-odd nuclei in the nuclear chart by overcoming all possible challenges.
- ✓ To construct the first relativistic nuclear mass table with the deformation and continuum effects by the DRHBc theory.
- ✓ To explore novel phenomena in nuclear physics by the DRHBc theory and various applications of the DRHBc mass table in nuclear astrophysics.
- ✓ To promote and strengthen an active scientific collaboration in the fields of nuclear physics and nuclear astrophysics between the parties.

https://drhbctable.jcnp.org/

Dripline v.s. deformation

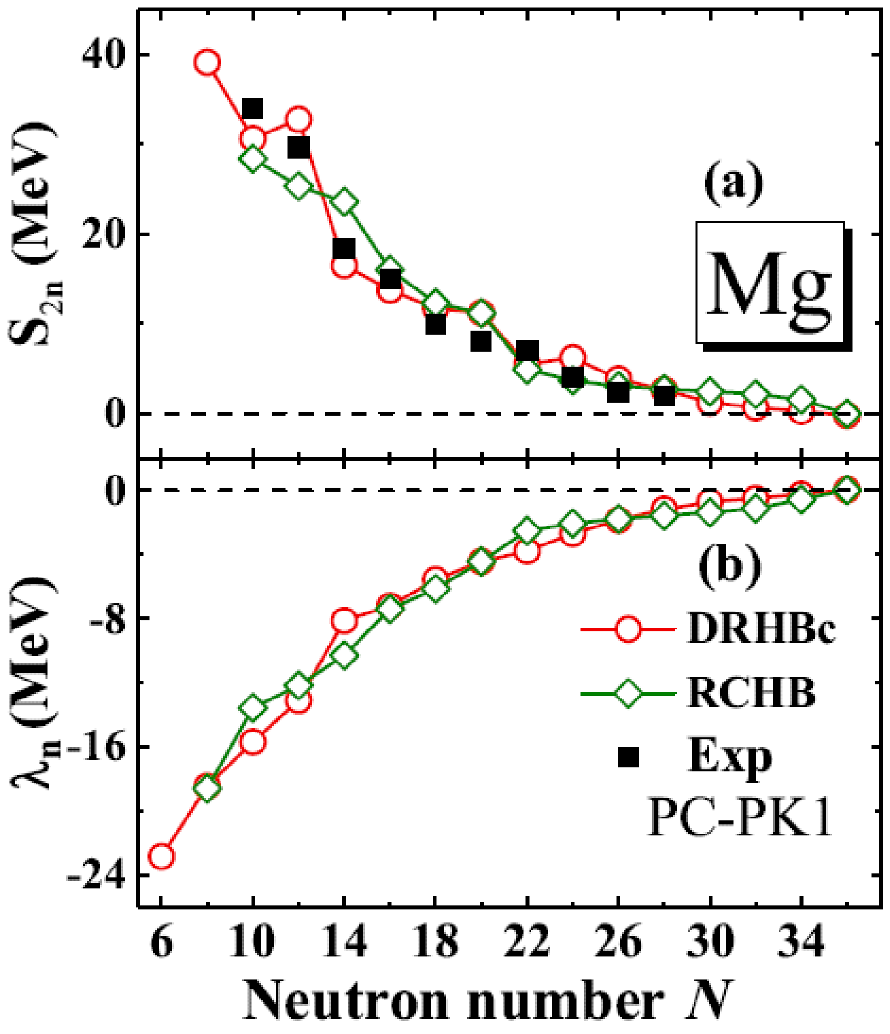

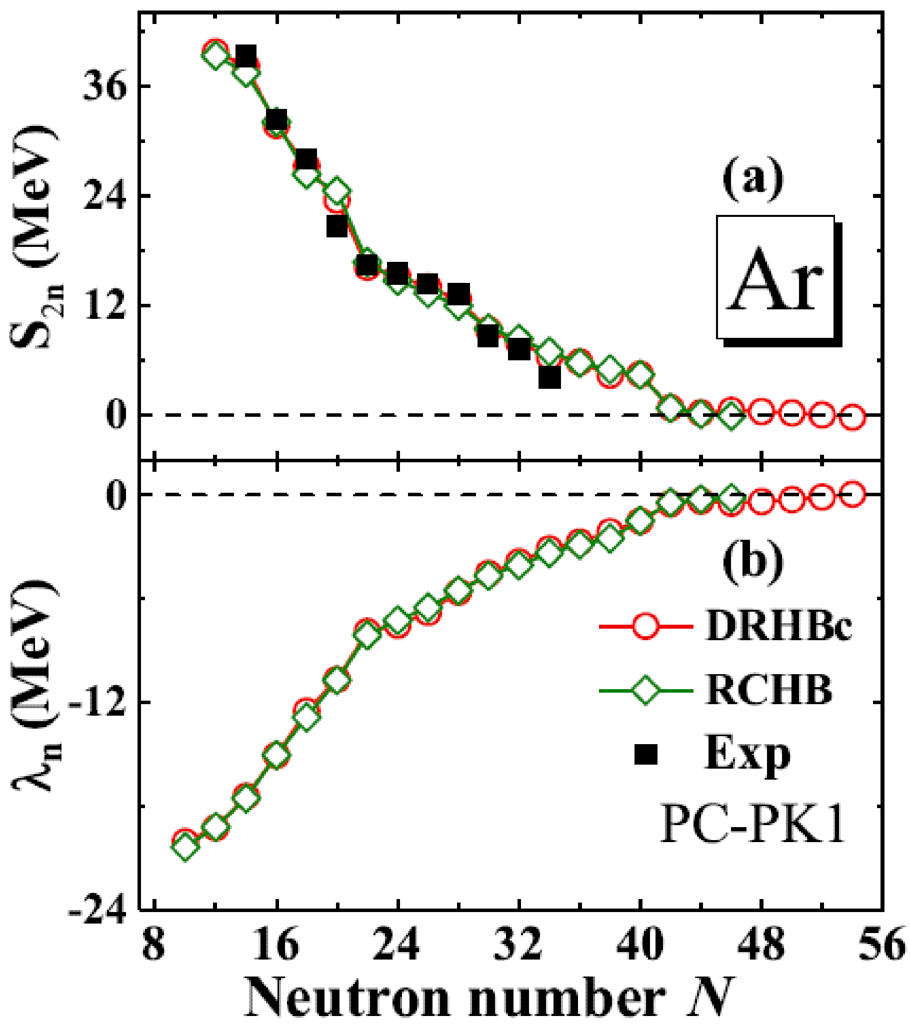

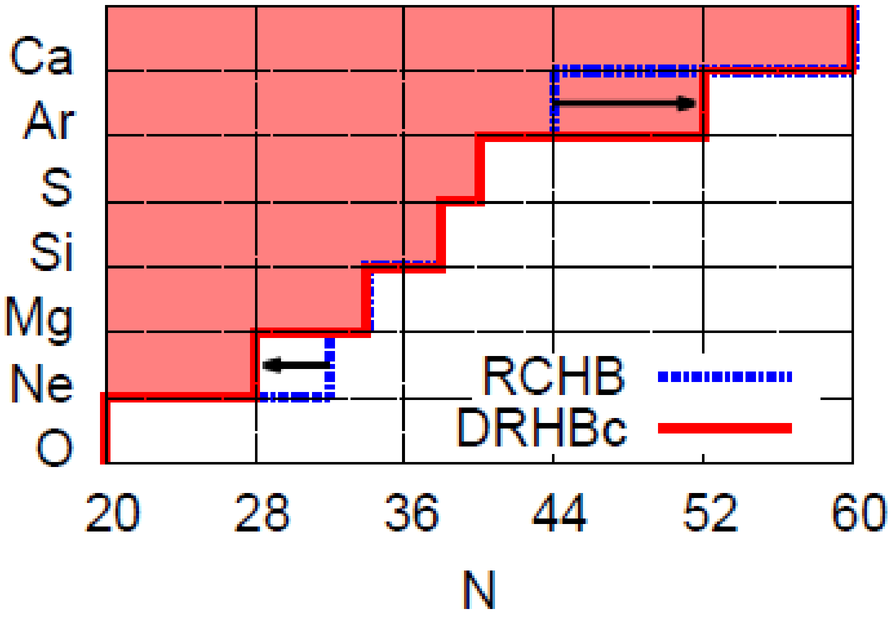

•

Element (Z)	neutron number (N)	
	RCHB	DRHBc
O (8)	20	20
Ne (10)	32	28
Mg (12)	34	34
Si (14)	38	38
S (16)	40	40
Ar (18)	44	52
Ca (20)	60	60

Eun Jin In, YK et al, Int.J.Mod.Phys.E 30 (2021) 2150009

Shape coexistence

In density functional theory, shape coexistence is closely linked to the existence of degenerate vacua. This raises the question: How small is "small" in the context of degenerate vacua? We can roughly estimate this small energy difference using the uncertainty principle. Taking $\Delta x \cdot \Delta p \approx \hbar/2$ with a nuclear diameter $\Delta x \approx 2.5A^{1/3}$ fm, we can estimate the energy uncertainty as $\Delta E \approx (\Delta p)^2/2m \approx 3.3/A^{2/3}$ MeV $\approx 100-300$ keV for most nuclei. Therefore, in the context of density functional theory, we can consider an energy difference of a few hundred keV to be "small".

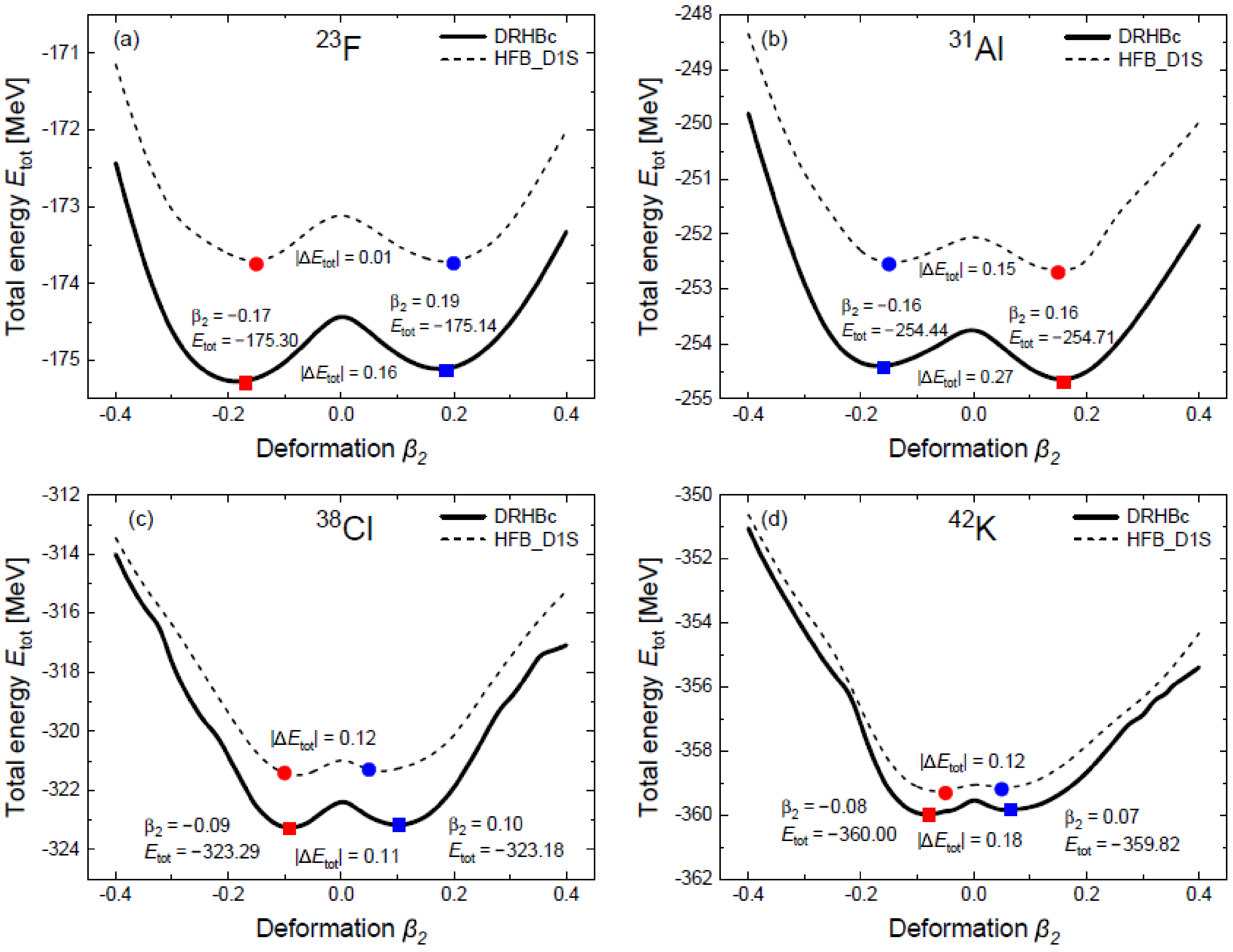

(a)
23F
DRHBc
HFB_D1S
|ΔEtot| = 0.01
β2 = 0.19
Etot = −175.14
β2 = −0.17
Etot = −175.30
|ΔEtot| = 0.16
(b)
31Al
DRHBc
HFB_D1S
|ΔEtot| = 0.15
β2 = −0.16
Etot = −254.44
β2 = 0.16
Etot = −254.71
|ΔEtot| = 0.27
(c)
38Cl
DRHBc
HFB_D1S
|ΔEtot| = 0.12
β2 = −0.09
Etot = −323.29
|ΔEtot| = 0.11
β2 = 0.10
Etot = −323.18
(d)
42K
DRHBc
HFB_D1S
|ΔEtot| = 0.12
β2 = −0.08
Etot = −360.00
|ΔEtot| = 0.18
β2 = 0.07
Etot = −359.82
Total energy Etot [MeV]
Deformation β2

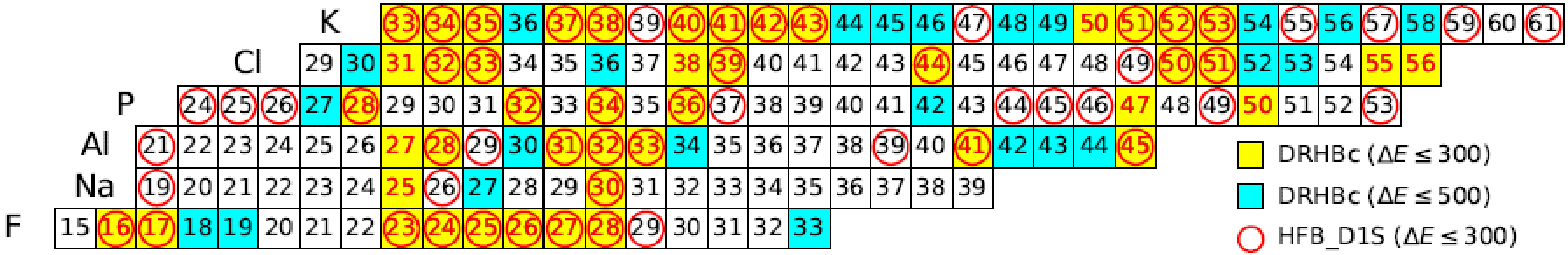

K
Cl
P
Al
Na
F
DRHBc (ΔE ≤ 300)
DRHBc (ΔE ≤ 500)
HFB_D1S (ΔE ≤ 300)

Bubble nuclei

Missing protons

The calculated proton density for silicon-34 (right) and, for comparison, sulfur-36 (left), as a function of the distance from the center of the nucleus. At its center, silicon-34 has about half the proton density of a comparable nucleus.

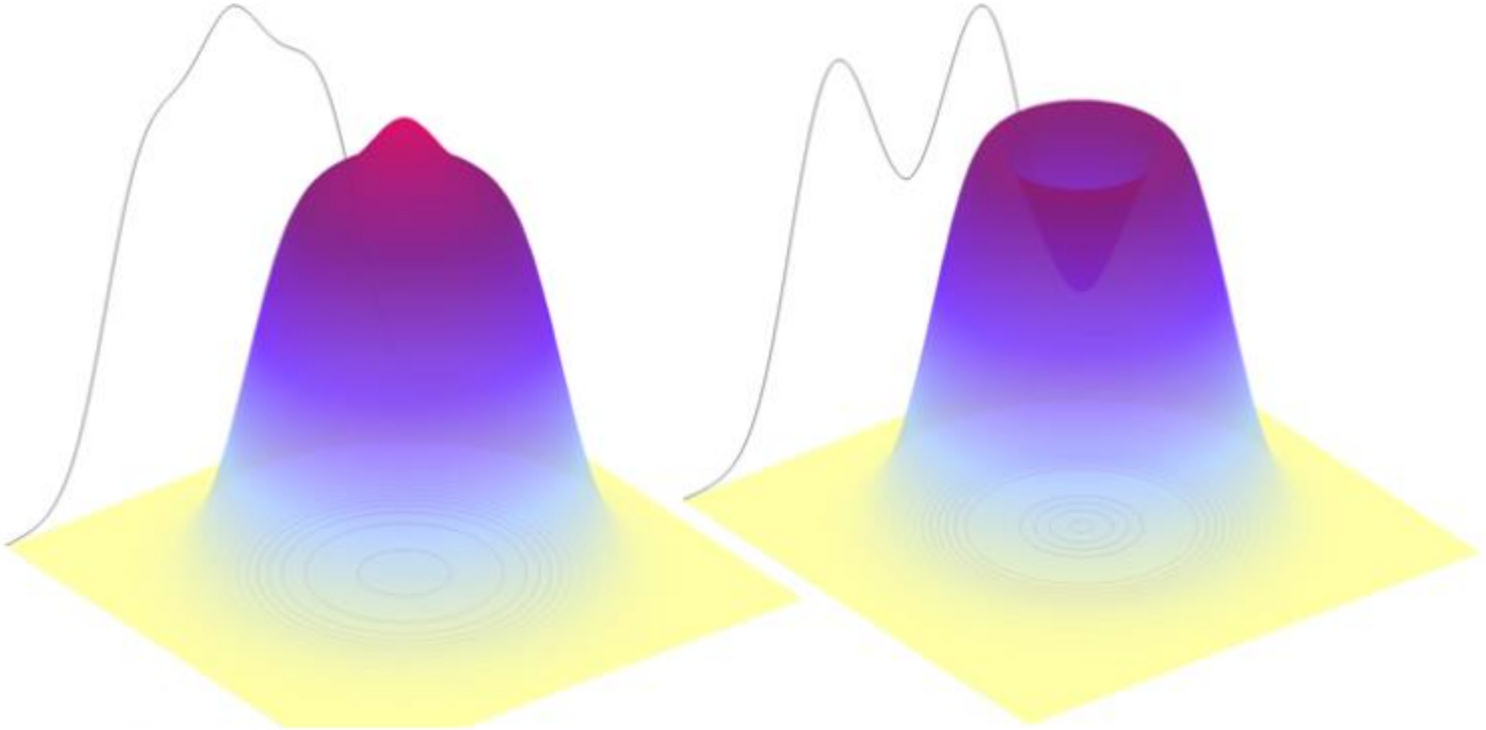

J.-P. EBRAN

The unstable isotope silicon-34 has a bubblelike center with a paucity of protons, scientists report October 24 in *Nature Physics*.

ScienceNews
INDEPENDENT JOURNALISM SINCE 1921

OCTOBER 24, 2016

proton depletion fraction

$$\mathcal{B}_p \equiv \left(1 - \frac{\rho_{p,\mathrm{c}}}{\rho_{p,\mathrm{max}}}\right) \times 100\,[\%].$$

$$\bar{\rho}_{p,\mathrm{max}} = \frac{\int \rho_p(r,\theta)\delta(r - r_{\mathrm{max}}(\theta))dV}{\int \delta(r - r_{\mathrm{max}}(\theta))dV}$$

$$\mathcal{B}_p^{\star} \equiv \left(1 - \frac{\rho_{p,\mathrm{c}}}{\bar{\rho}_{p,\mathrm{max}}}\right) \times 100\%$$

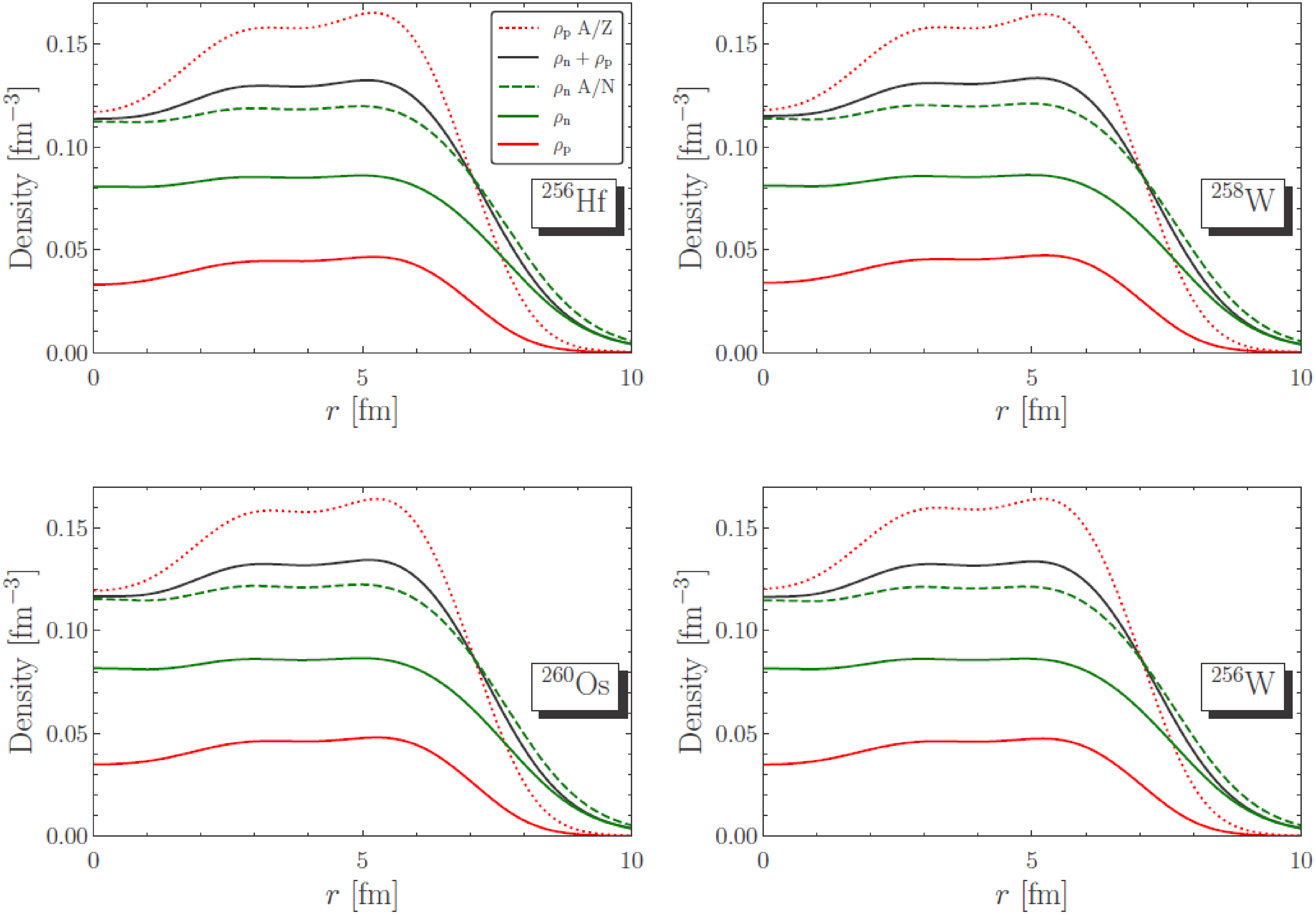

ρ_p A/Z
$\rho_n + \rho_p$
ρ_n A/N
ρ_n
ρ_p
^{256}Hf
^{258}W
^{260}Os
^{256}W
Density [fm^{-3}]
0.00
0.05
0.10
0.15
0
5
10
r [fm]

	DRHBc		RCHB
Nucleus	β_2	$\mathcal{B}_p^\star$ [%]	$\mathcal{B}_p^\star(=\mathcal{B}_p)$ [%]
^{256}Hf	0.000	29.2	27.4
^{258}W	0.000	28.3	26.6
^{260}Os	0.000	27.2	25.5
^{256}W	0.000	26.7	25.1
^{258}Os	0.000	26.0	24.3
^{254}Hf	0.057	25.7	25.7
^{200}Hf	0.000	25.6	24.8
^{198}Hf	0.000	25.3	24.5
^{262}Pt	0.000	25.2	23.5
^{202}W	0.000	25.1	24.3

TABLE III. List of the isotopes with both bubble structure and shape coexistence. $|\Delta E|$ is the absolute value of the energy difference between prolate and oblate shapes.

	Prolate shape		Oblate shape		
Nucleus	β_2	$\mathcal{B}^{\star}_p$ [%]	β_2	$\mathcal{B}^{\star}_p$ [%]	$\lvert\Delta E\rvert$[MeV]
^{202}Hf	+0.100	23.7	−0.072	22.4	0.214
^{234}Hf	+0.272	20.5	−0.234	2.4	0.263
^{236}Hf	+0.262	20.4	−0.227	2.2	0.318
^{240}Hf	+0.241	21.0	−0.192	3.5	0.468
^{250}Hf	+0.091	24.0	−0.086	18.3	0.171
^{194}W	+0.136	23.1	−0.126	12.1	0.155
^{204}W	+0.080	23.8	−0.060	22.8	0.087
^{254}W	+0.068	24.2	−0.060	21.7	0.401
^{196}Os	+0.123	23.6	−0.119	11.0	0.096
^{206}Os	+0.044	24.1	−0.042	23.5	0.006
^{208}Os	+0.112	22.4	−0.079	20.4	0.447
^{256}Os	+0.058	24.0	−0.065	20.6	0.141
^{210}Pt	+0.072	22.5	−0.061	21.4	0.016
^{212}Pt	+0.113	21.0	−0.080	19.6	0.404

Y.-B. Choi, C.-H. Lee, M.-H. Mun, YK, *Bubble nuclei with shape coexistence in even-even isotopes of Hf to Hg*, Phys. Rev. C 105 (2022) 024306

Alpha decay

$$T_{1/2} = \frac{\hbar \ln 2}{\Gamma},$$
$$\Gamma = P_\alpha N_\mathrm{f} \frac{\hbar^2}{4\mu} P_\mathrm{total},$$

$$P_\alpha = \frac{2S_\mathrm{p} + 2S_\mathrm{n} - S_\alpha}{S_\alpha}$$

$$S_\mathrm{p}(Z,N) = E_\mathrm{b}(Z,N) - E_\mathrm{b}(Z-1,N),$$
$$S_\mathrm{n}(Z,N) = E_\mathrm{b}(Z,N) - E_\mathrm{b}(Z,N-1),$$
$$S_\alpha(Z,N) = E_\mathrm{b}(Z,N) - E_\mathrm{b}(Z-2,N-2)$$

total penetration probability with the WKB approximation

Preformation factor from cluster-formation model

Preformation factor from NLEFT?

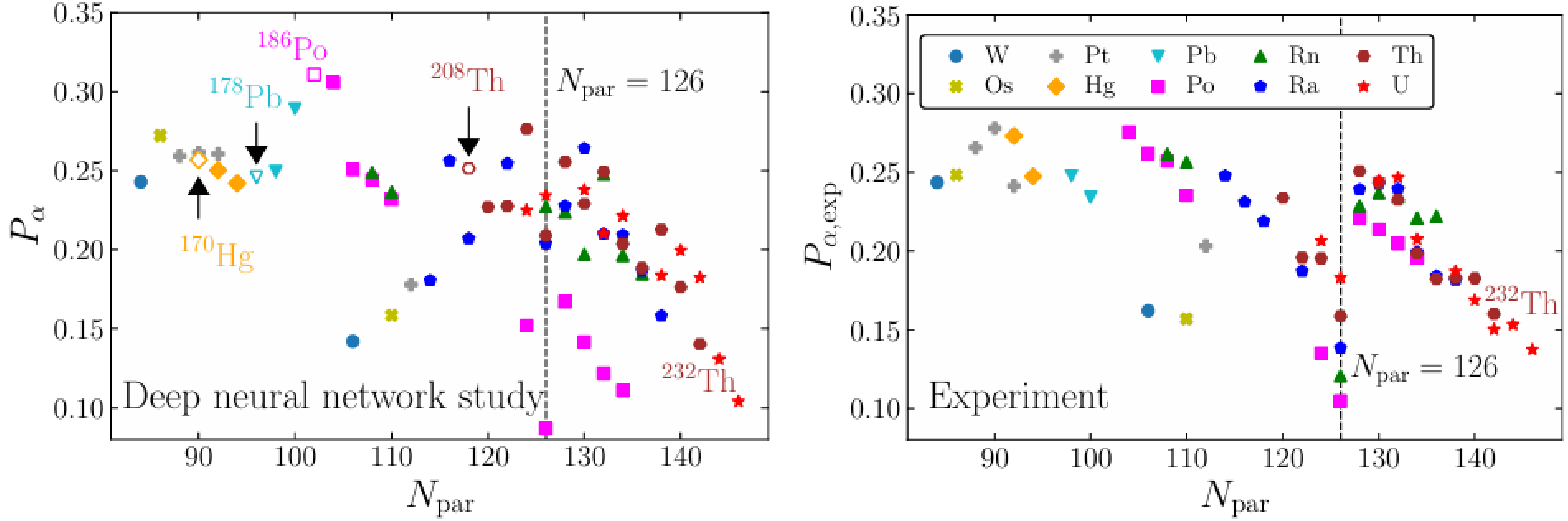

(a) (b)

Preformation factors as a function of parent neutron number

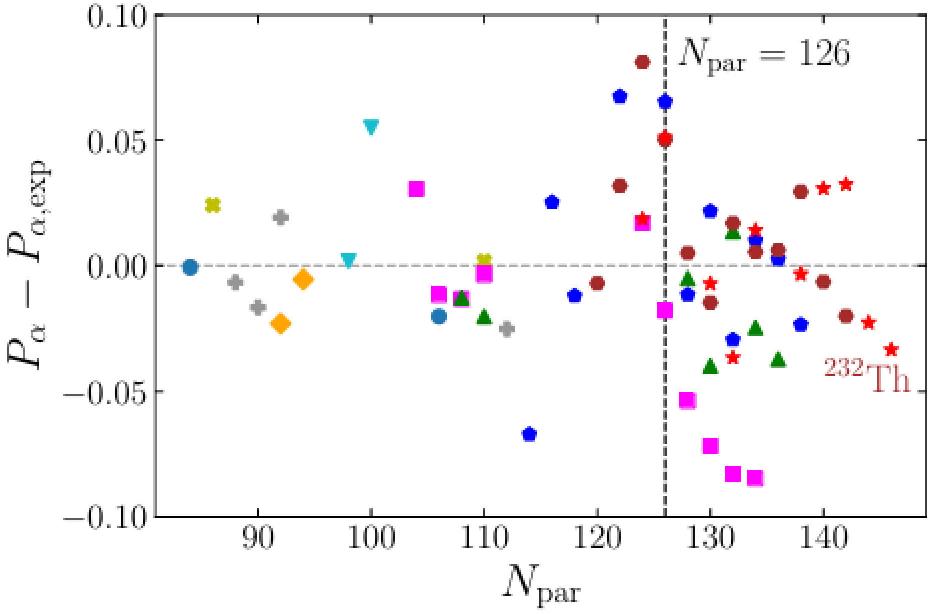

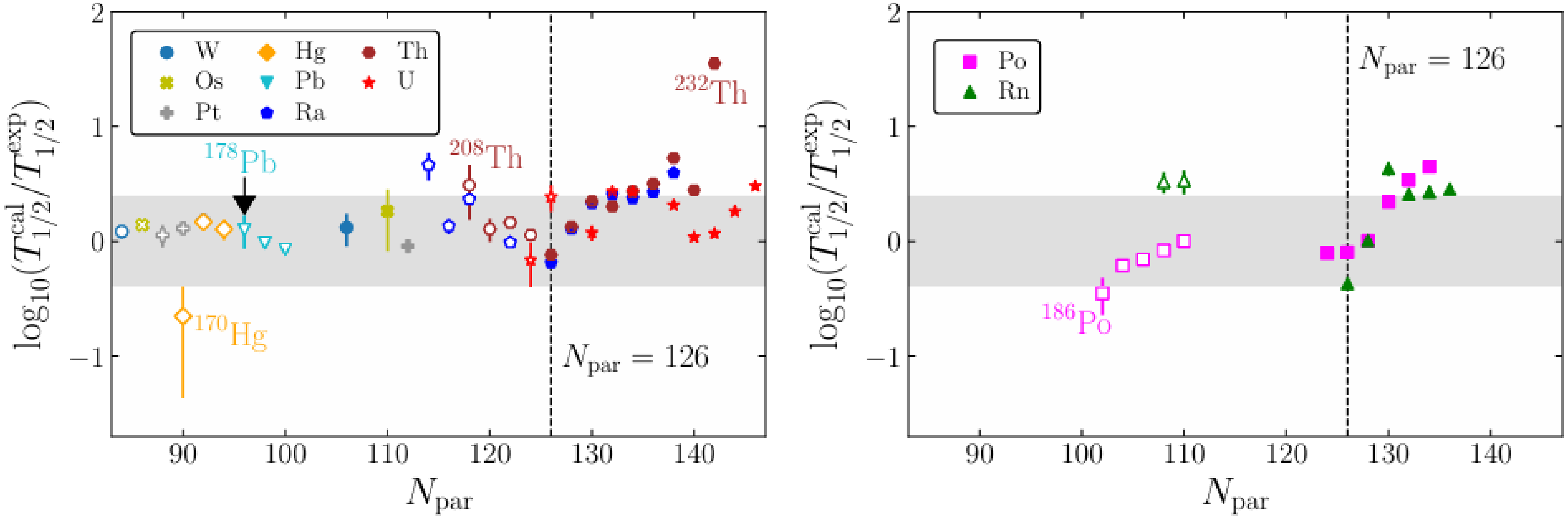

W
Os
Pt
Hg
Pb
Ra
Th
U
^{178}Pb
^{208}Th
^{232}Th
^{170}Hg
$N_{\mathrm{par}} = 126$
$\log_{10}(T^{\mathrm{cal}}_{1/2}/T^{\mathrm{exp}}_{1/2})$
N_{par}
Po
Rn
^{186}Po

Halos

^{37}Mg was identified as a halo nucleus in 2014 and remains the heaviest nuclear halo system to date, its description has been still challenging afterwards.

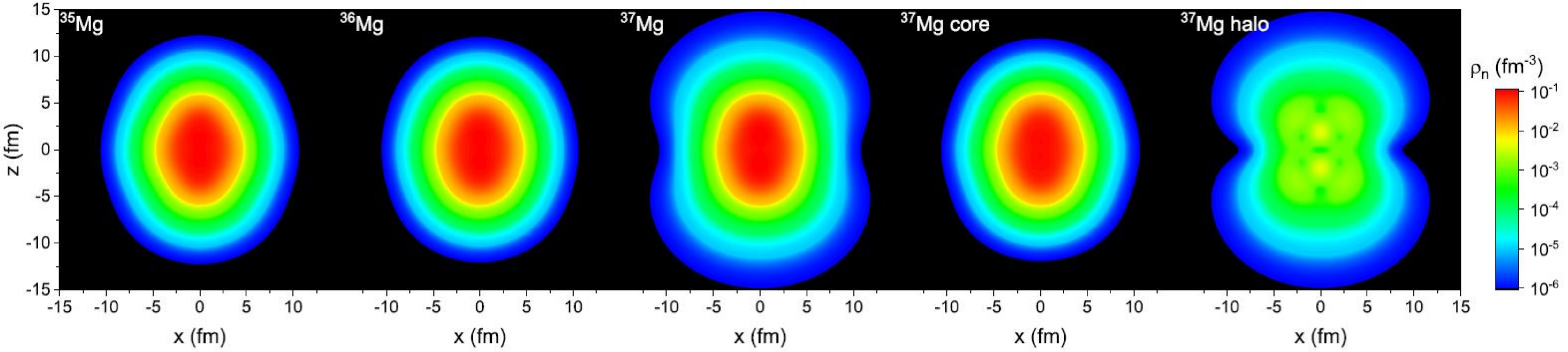

K.Y. Zhang, S.Q. Yang, J.L. An, S.S. Zhang, P. Papakonstantinou, M.-H. Mun, YK, H. Yan,   PLB 844 (2023) 138112

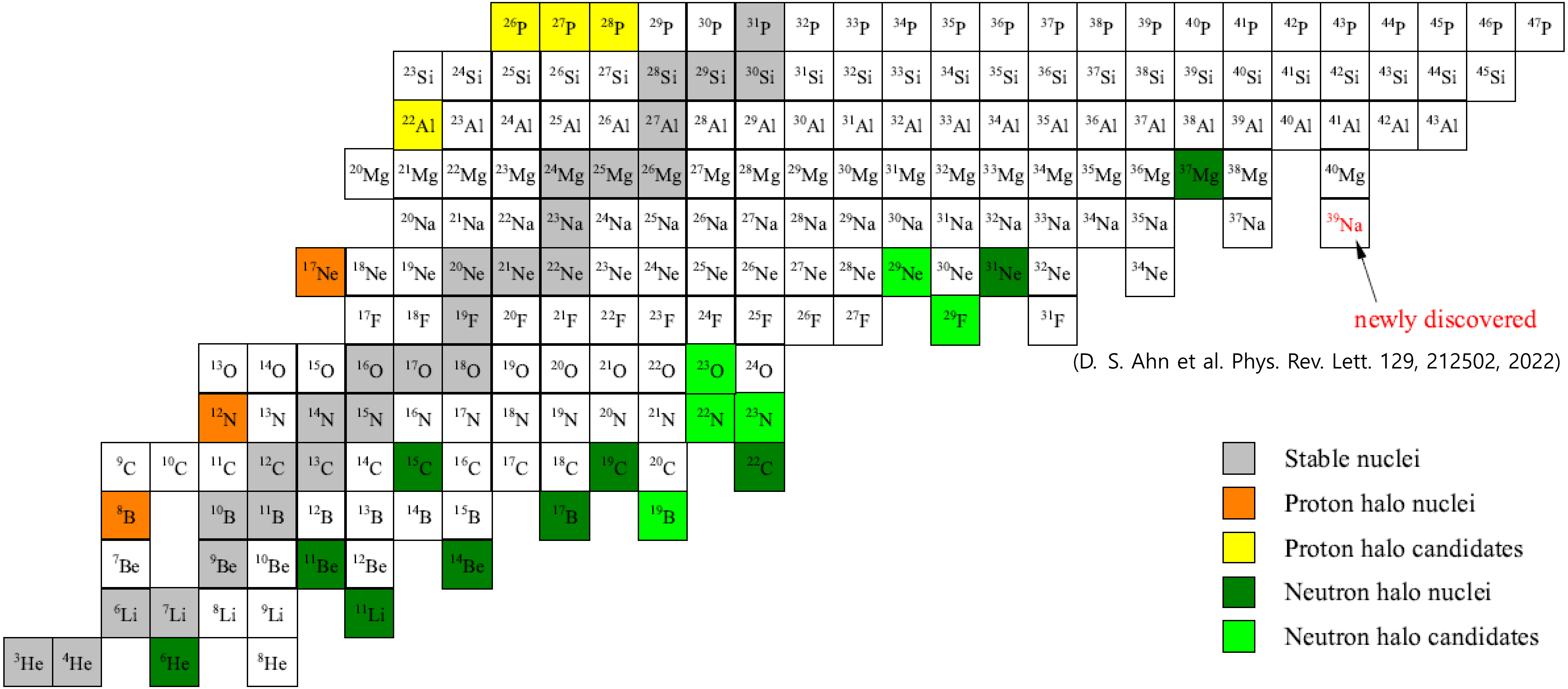
^{26}P ^{27}P ^{28}P ^{29}P ^{30}P ^{31}P ^{32}P ^{33}P ^{34}P ^{35}P ^{36}P ^{37}P ^{38}P ^{39}P ^{40}P ^{41}P ^{42}P ^{43}P ^{44}P ^{45}P ^{46}P ^{47}P
^{23}Si ^{24}Si ^{25}Si ^{26}Si ^{27}Si ^{28}Si ^{29}Si ^{30}Si ^{31}Si ^{32}Si ^{33}Si ^{34}Si ^{35}Si ^{36}Si ^{37}Si ^{38}Si ^{39}Si ^{40}Si ^{41}Si ^{42}Si ^{43}Si ^{44}Si ^{45}Si
^{22}Al ^{23}Al ^{24}Al ^{25}Al ^{26}Al ^{27}Al ^{28}Al ^{29}Al ^{30}Al ^{31}Al ^{32}Al ^{33}Al ^{34}Al ^{35}Al ^{36}Al ^{37}Al ^{38}Al ^{39}Al ^{40}Al ^{41}Al ^{42}Al ^{43}Al
^{20}Mg ^{21}Mg ^{22}Mg ^{23}Mg ^{24}Mg ^{25}Mg ^{26}Mg ^{27}Mg ^{28}Mg ^{29}Mg ^{30}Mg ^{31}Mg ^{32}Mg ^{33}Mg ^{34}Mg ^{35}Mg ^{36}Mg ^{37}Mg ^{38}Mg ^{40}Mg
^{20}Na ^{21}Na ^{22}Na ^{23}Na ^{24}Na ^{25}Na ^{26}Na ^{27}Na ^{28}Na ^{29}Na ^{30}Na ^{31}Na ^{32}Na ^{33}Na ^{34}Na ^{35}Na ^{37}Na ^{39}Na
^{17}Ne ^{18}Ne ^{19}Ne ^{20}Ne ^{21}Ne ^{22}Ne ^{23}Ne ^{24}Ne ^{25}Ne ^{26}Ne ^{27}Ne ^{28}Ne ^{29}Ne ^{30}Ne ^{31}Ne ^{32}Ne ^{34}Ne
^{17}F ^{18}F ^{19}F ^{20}F ^{21}F ^{22}F ^{23}F ^{24}F ^{25}F ^{26}F ^{27}F ^{29}F ^{31}F
newly discovered
(D. S. Ahn et al. Phys. Rev. Lett. 129, 212502, 2022)
^{13}O ^{14}O ^{15}O ^{16}O ^{17}O ^{18}O ^{19}O ^{20}O ^{21}O ^{22}O ^{23}O ^{24}O
^{12}N ^{13}N ^{14}N ^{15}N ^{16}N ^{17}N ^{18}N ^{19}N ^{20}N ^{21}N ^{22}N ^{23}N
^{9}C ^{10}C ^{11}C ^{12}C ^{13}C ^{14}C ^{15}C ^{16}C ^{17}C ^{18}C ^{19}C ^{20}C ^{22}C
^{8}B ^{10}B ^{11}B ^{12}B ^{13}B ^{14}B ^{15}B ^{17}B ^{19}B
^{7}Be ^{9}Be ^{10}Be ^{11}Be ^{12}Be ^{14}Be
^{6}Li ^{7}Li ^{8}Li ^{9}Li ^{11}Li
^{3}He ^{4}He ^{6}He ^{8}He
Stable nuclei
Proton halo nuclei
Proton halo candidates
Neutron halo nuclei
Neutron halo candidates

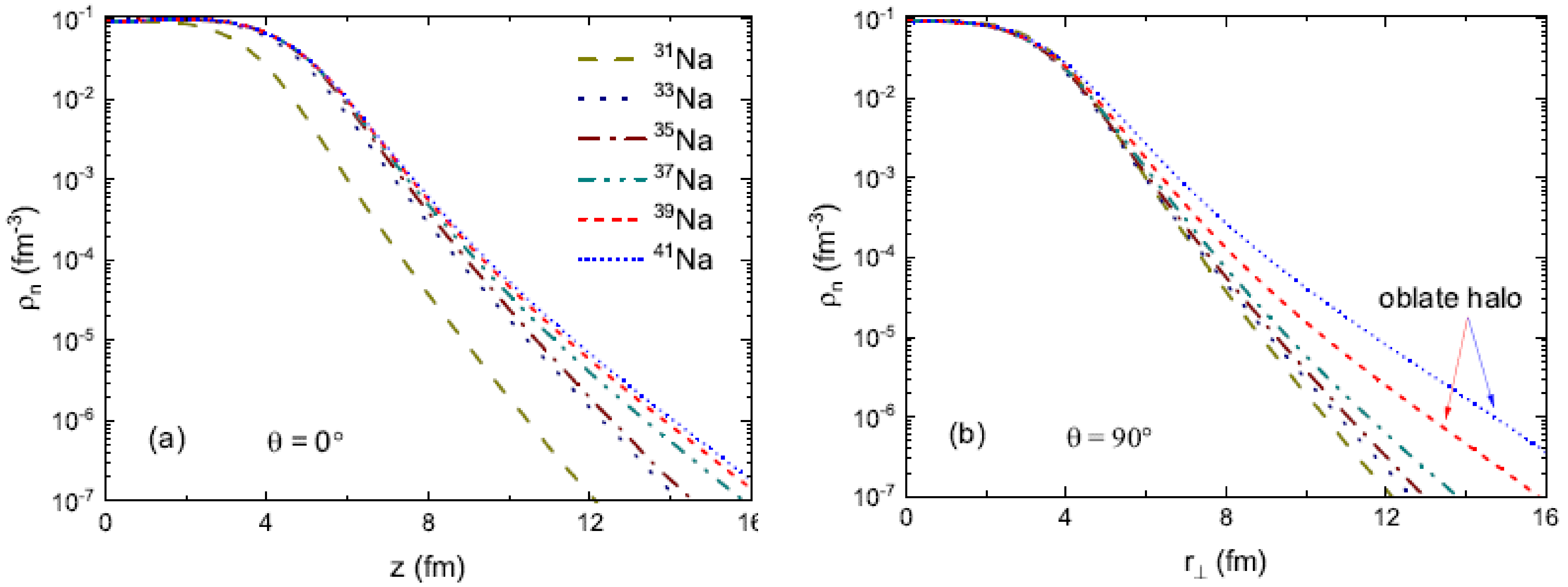

K.Y. Zhang, P. Papakonstantinou, M.-H. Mun, Y. Kim, H. Yan et al. Phys. Rev. C 107 (2023) 4, L041303

ELSEVIER

Atomic Data and Nuclear Data Tables

Volume 144, March 2022, 101488

Nuclear mass table in deformed relativistic Hartree–Bogoliubov theory in continuum, I: Even–even nuclei

Kaiyuan Zhang [a], Myung-Ki Cheoun [b], Yong-Beom Choi [c], Pooi Seong Chong [d], Jianmin Dong [e f], Zihao Dong [a], Xiaokai Du [a], Lisheng Geng [g h], Eunja Ha [i], Xiao-Tao He [j], Chan Heo [d], Meng Chit Ho [d], Eun Jin In [k l], Seonghyun Kim [b], Youngman Kim [m], Chang-Hwan Lee [c], Jenny Lee [d], Hexuan Li [a], Zhipan Li [n], Tianpeng Luo [a], Jie Meng [a], Myeong-Hwan Mun [b o], Zhongming Niu [p], Cong Pan [a], Panagiota Papakonstantinou [m], Xinle Shang [e f], Caiwan Shen [q], Guofang Shen [g], Wei Sun [n], Xiang-Xiang Sun [r s], Chi Kin Tam [d], Thaivayongnou [g], Chen Wang [j], Xingzhi Wang [a], Sau Hei Wong [d], Jiawei Wu [j], Xinhui Wu [a], Xuewei Xia [t], Yijun Yan [e f], Ryan Wai-Yen Yeung [d], To Chung Yiu [d], Shuangquan Zhang [a], Wei Zhang [h], Xiaoyan Zhang [p], Qiang Zhao [k a], Shan-Gui Zhou [s u v w], DRHBc Mass Table Collaboration

ELSEVIER

Atomic Data and Nuclear Data Tables

Volume 158, July 2024, 101661

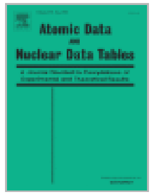

Nuclear mass table in deformed relativistic Hartree–Bogoliubov theory in continuum, II: Even-Z nuclei

Peng Guo [1], Xiaojie Cao [2], Kangmin Chen [3], Zhihui Chen [4], Myung-Ki Cheoun [5], Yong-Beom Choi [6], Pak Chung Lam [4], Wenmin Deng [7], Jianmin Dong [8 9], Pengxiang Du [10], Xiaokai Du [11], Kangda Duan [8], Xiaohua Fan [11], Wei Gao [12], Lisheng Geng [13 14 15 16], Eunja Ha [17], Xiao-Tao He [18], Jinniu Hu [19], Jingke Huang [12], Kun Huang [18], Yanan Huang [20], Zidan Huang [12], Kim Da Hyung [4], Hoi Yat Chan [4], Xiaofei Jiang [1], Seonghyun Kim [5], Youngman Kim [21], Chang-Hwan Lee [6], Jenny Lee [4], Jian Li [10], Minglong Li [22], Zhipan Li [11], Zhengzheng Li [1], Zhanjiang Lian [23], Haozhao Liang [22 24], Lang Liu [25], Xiao Lu [26], Zhi-Rui Liu [18], Jie Meng [1], Ziyan Meng [1], Myeong-Hwan Mun [5], Yifei Niu [20], Zhongming Niu [27], Cong Pan [28 1], Jing Peng [7], Xiaoying Qu [3], Panagiota Papakonstantinou [29], Tianshuai Shang [10], Xinle Shang [8 9], Caiwan Shen [30], Guofang Shen [13], Tingting Sun [12], Xiang-Xiang Sun [31 26], Sibo Wang [32], Tianyu Wang [33], Yiran Wang [2], Yuanyuan Wang [34], Jiawei Wu [18], Liang Wu [12], Xinhui Wu [35], Xuewei Xia [36], Huihui Xie [10], Jiangming Yao [37 38], Kwan Yau Ip [4], To Chung Yiu [4], Jianghan Yu [30], Yangyang Yu [3], Kaiyuan Zhang [39 1], Shijie Zhang [12], Shuangquan Zhang [1], Wei Zhang [12], Xiaoyan Zhang [27], Yanxin Zhang [37], Ying Zhang [2], Yingxun Zhang [23 40], Zhenhua Zhang [34], Qiang Zhao [21], Yingchun Zhao [1], Ruyou Zheng [13], Chang Zhou [1], Shan-Gui Zhou [26 41 31 14], Lianjian Zou [19], DRHBc Mass Table Collaboration

DRHBc mass table project

Nuclear mass table in deformed relativistic Hartree–Bogoliubov theory in continuum, II: Even-Z nuclei

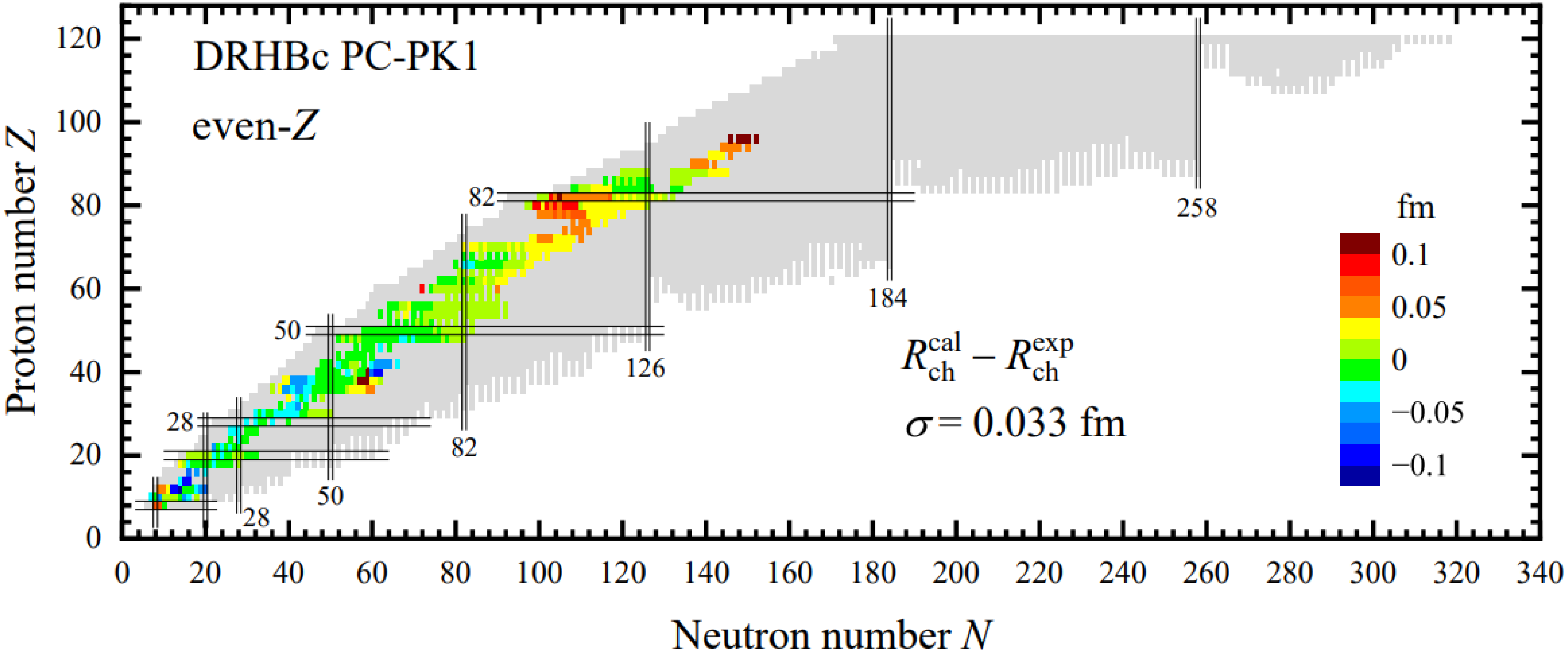

4829 bound even-Z nuclei from O(Z=8) to Z=120 predicted by the DRHBc theory with PC-PK1.
For the 620 even-Z nuclei (8 ≤ Z ≤ 120) with charge radius measured, the deviations between the DRHBc calculations with PC-PK1 and the data are scaled by colors.

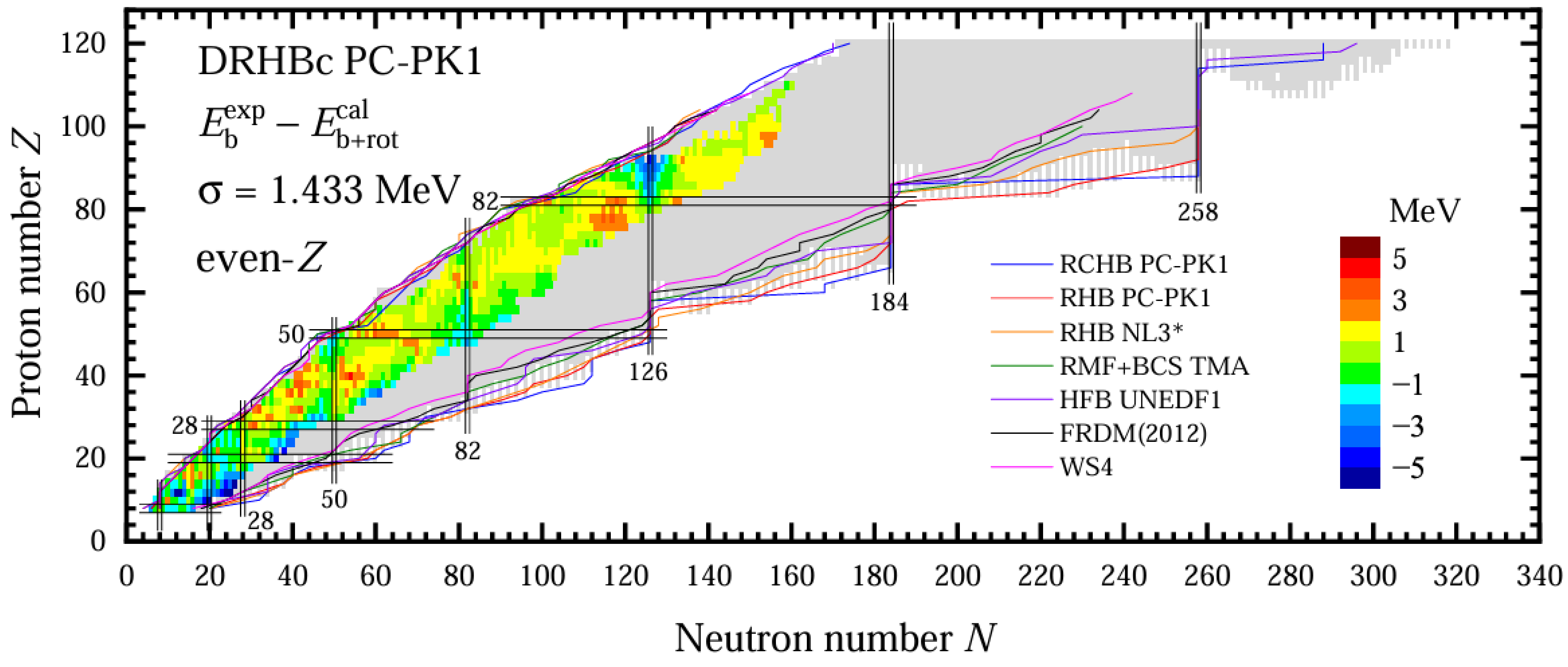

For the1244 even-Z nuclei with mass measured, the binding energy differences between the data and the DRHBc calculations are scaled bycolors.

- It may be interesting if one can clearly pin down the location of the neutron dripline and describe exotic nuclear shapes in NLEFT.

  - ✓ Clustering (d, t, ^{3}He, alpha) in NLEFT?   right after this meeting with M. Kim and S. Shen@BUAA

ONOKORO project

❖ A new project ONOKORO (RCNP, RIKEN, HIMAC)

- **To investigate clustering in medium-to heavy mass nuclei with cluster knock-out reactions**

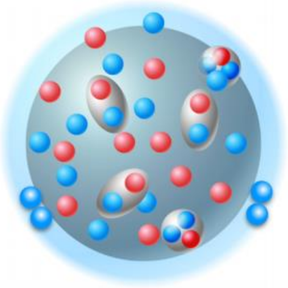

(d, t, ^{3}He, α) cluster formation in a nucleus

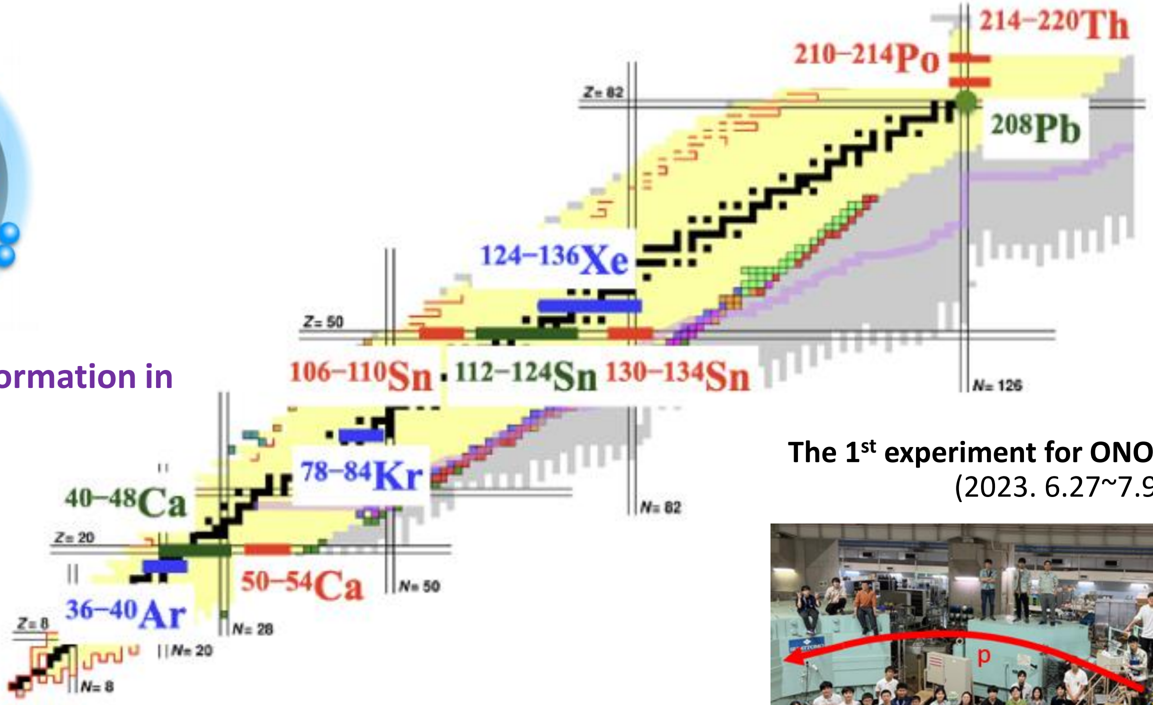

(p,pX) @ E/A = 200—300 MeV (X: d, t, 3He, α)

The 1st experiment for ONOKORO project
(2023. 6.27~7.9)

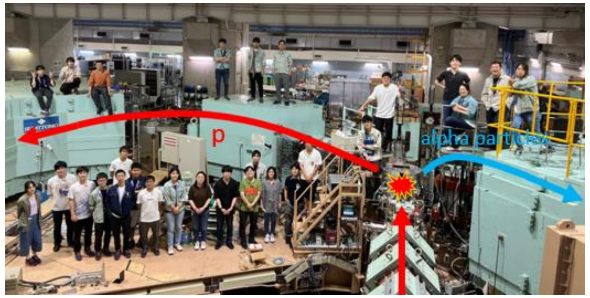

A new detector array, TOGAXSI
- GAGG:Ce scintillators and silicon-strip detectors

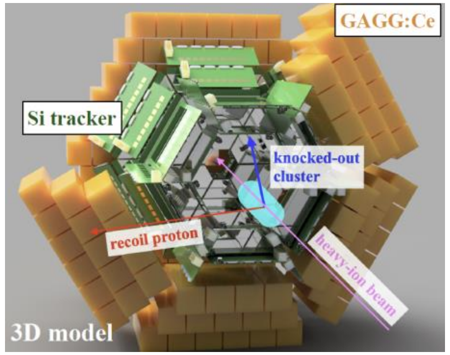

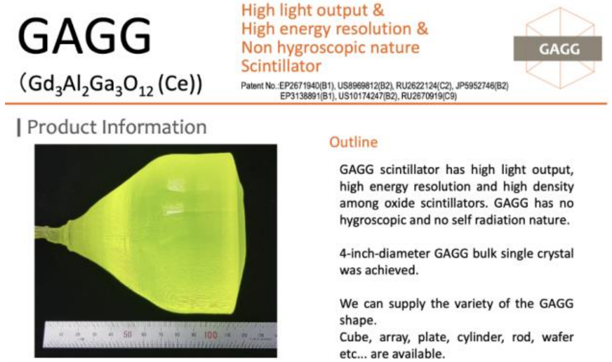

❖ Relative abundances of d,t,^{3}He,α clusters and their isotopic dependences
❖ Surface α formation in heavy nuclei→ understanding of α-decay
❖ Discovery of deuteron clusters in heavy nuclei
❖ First determination of the ratio of t/^{3}He clusters

The first generation of the TOGAXSI will be ready by the end of 2024, including the 10 GAGG:Ce scintillators provided by CENS.